Original Article

Mechanical properties of resin glass fiber-reinforced abutment in comparison to titanium abutment

Mirko Andreasi Bassi, Rossella Bedini,[1] Raffella Pecci,[1] Pietro Ioppolo,[1] Dorina Lauritano,[2] Francesco Carinci[3]

Department of Technologies and Health, Superior Institute of Health, Biomaterials and Contaminants Section, Superior Institute of Health, Rome, Italy, [1]Department of Technologies and Health, Biomaterials and Contaminants Section, Superior Institute of Health, Rome, [2]Centre of Neuroscience Milan NeuroMi, University of Milan-Bicocca, [3]Department of Morphology and Oral and Maxillofacial Surgery, Surgery and Experimental Medicine, University of Ferrara, Ferrara, Italy

Address for correspondence:
Dr. Dorina Lauritano, Department of Translational Surgery and Medicine, Centre of Neuroscience of Milan, University of Milan-Bicooca, NeuroMI, Via Cadore 48, 20052 Monza (MB), Italy. E-mail: dorina.lauritano@ unimib.it

Abstract:

Purpose: So far, definitive implant abutments have been performed with high elastic modulus materials, which prevented any type of shock absorption of the chewing loads and as a consequence, the protection of the bone-fixture interface. This is particularly the case when the esthetic restorative material chosen is ceramic rather than composite resin. The adoption of an anisotropic abutment, characterized by an elastic deformability, could allow decreasing the impulse of chewing forces transmitted to the crestal bone. **Materials and Methods:** According to research protocol, the mechanical resistance to cyclical load was evaluated in a tooth-colored fiber-reinforced abutment (TCFRA) prototype and compared to that of a titanium abutment (TA), thus eight TCFRAs and eight TAs were adhesively cemented on as many titanium implants. The swinging that the two types of abutments showed during the application of sinusoidal load was also analyzed. **Results:** In the TA group, both fracture and deformation occurred in 12.5% of samples while debonding 62.5%. In the TCFRA group, only debonding was present in 37.5% of samples. In comparison to the TAs, the TCFRAs exhibited a greater swinging during the application of sinusoidal load. In the TA group, the extrusion prevailed, whereas in the TCFRA group, the intrusion was more frequent. **Conclusion:** The greater elasticity of TCFRA to the flexural load allows absorbing part of the transversal load applied on the fixture during the chewing function, thus reducing the stress on the bone-implant interface.

Key words:
Abutment, cyclical load, dental implants, fatigue test, fiber-reinforced, periodontal ligament

INTRODUCTION

The clinical success and longevity of endosseous implants, after their prosthetic finalization, mainly depends on mechanical factors. It is shown that an excessive mechanical stress can be cause of initial bone loss around implants in the presence of a rigid implant-prosthetic connection.[1]

When compared to an implant, the periodontal ligament (PL) of a natural tooth helps reducing the forces transmitted to the crestal bone.[2] The PL, working as a viscoelastic shock absorber, is able to reduce the extent of stress to the bone, lengthening the time in which the load is dissipated, therefore, decreasing the impulse of the force.[3] Compared to the PL, the bone interface of an implant is not as resilient, and the forces generated by the occlusal loading are not dissipated completely but rather transmitted to the adjacent bone, with a greater intensity. The teeth also have the advantage compared to implants to possess a finer proprioception manifested through the ability to perceive even minimal occlusal strain and stress.[4,5]

Therefore, in the case of an implant-supported prosthesis, the patient with the risk of an excessive peri-implant bone resorption may perceive not every occlusal overload.[4,5] In addition, a force of the same magnitude may have incredibly different effects at the bone interface, according to the direction of the applied load. The greater the angle of the force, relative to the axis of the implant body, the greater the resulting potential damage to the bony crest.[6-10]

In the case of a titanium implant-bone system, the bone has the lower modulus of elasticity. In fact, titanium is about 5 times stiffer than cortical bone, creating the conditions for bone resorption if the stress at the interface is excessive.[9-11] Treatment plans should provide methods for reducing stress so that the initial loss of bone is less likely to occur.[12]

There are several techniques to improve the biomechanical condition of the transosseous implant region, lowering the stress on the crestal bone. The stress can be reduced by increasing the implant surface or decreasing the biomechanical forces that may be decreased in magnitude, duration, type, direction, and application.[6,12] Another possible method to reduce the stress at the crestal bone level is to use an abutment made of a flexible material that deforms within its elastic limit, absorbing a part of the load applied.

The implant abutments are manufactured with high elastic modulus materials such as titanium,

steel, precious alloys, or esthetic ceramics.[13,14] These materials do not absorb any type of shock of the chewing loads and do not assure protection to the bone-fixture interface, especially when the aesthetic restorative material is ceramic rather than composite resin.[15,16] Some authors proposed to interpose a resilient support (teflon disk) between fixture and abutment, but this solution promoted the breakage of the locking screw of the abutment.[17]

The adoption of an abutment in composite material, reinforced with fibers parallel-oriented to its major axis, allows to decrease the impulse of chewing forces; this is possible thanks to the elastic deformation that the abutment would undergo, so increasing the time in which the load is dissipated. This anisotropic behavior would help to mitigate mainly the transverse and tensile components resulting from load applied to the implant body. Moreover, a resinous nature allows the adoption of an adhesive luting technique, which would contribute to the dissipation of chewing loads by reducing the concentration of stress on the bone-implant interface.[18] Other authors have proposed an aesthetic abutment made of composite material reinforced with unidirectional fibers as an alternative to all-ceramic abutments to be used in combination with metal-free crowns. Such abutment was tightened to the fixture by a metal screw. With some improvements, this abutment could be a promising alternative to conventional abutments and its fixation to the fixture by means of adhesive cementation could advantageously replace the connection via a screw.[19]

The purpose of this study was to investigate the mechanical performance, after cyclic stress, of a tooth-colored fiber-reinforced abutment (TCFRA) prototype and compare it with a titanium abutment (TA) of the same shape. Both abutments were adhesively cemented on the same type of titanium implants. The mechanical testing evaluated the excursion that the two types of abutments showed during the application of different sinusoidal load to assess the TCFRA performance to reduce the tensions and transverse forces transmitted to the bone.

MATERIALS AND METHODS

Eight TCFRAs were prototyped for this experimental work. The TCFRA abutment was composed of epoxy resin reinforced with pre-tensioned glass fibers. Eight TAs (Ti grade 2) with the same shape and dimension of TCFRAs were also chosen [Figure 1].

Sixteen cylindrical self-tapping titanium implants (L13 mm, Ø 3.8; Ti grade 2) were fixed on as many, trunk-conic form, self-curing acrylic resin supports (Resin Tray, Ravelli, Italy) through a specially made decomposable Denril™ mold.

Each implant was positioned with its long axis parallel to the major axis of the support. All the implants were placed in the resin supports up to the limit between the neck and the first coil of the implant screw. The abutment-implant connection adopted was a screwed internal hexagon (depth 6 mm, diameter 2.3 mm).

Both TCFRAs and TAs were adhesively cemented on as many implant-resin support systems, previously prepared.

In order to simulate the clinical situation in which the abutment is covered and protected by the crown, during the cyclical solicitation, a cylindrical brass cup has been cemented on
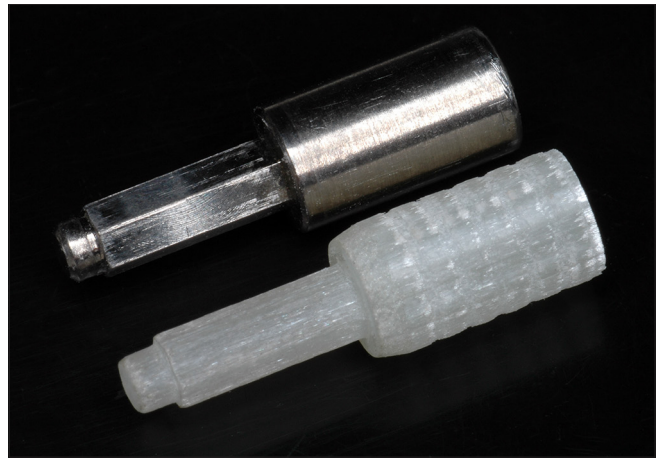

Figure 1: The titanium abutment and the experimental abutment

each abutment. For the fixation of both types of abutments to the fixtures and to the cylindrical brass cups, a composite cement (Panavia 21, Kuraray, Japan) has been used to ensure a valid bond with both no-precious metals adopted (titanium and brass) and the resinous matrix of the TCFRA. As regards the adhesive procedure, the bi-component adhesive system has been used associated to the composite cement (ED Primer, Kuraray, Japan). In order to optimize the micro-mechanical bond, the TAs and the inner surface of the cylindrical brass cups have been sandblasted with aluminum dioxide (average particle diameter: 177 μm) at 2 bar pressure. Both the cement and the adhesive have been used according to the manufacturer's instructions.

On each trunk-conic form acrylic resin support a vertical plane surface was applied with the purpose to allow a repeatable and reproducible orientation of the specimens both on the fatigue-testing machine and on the radiographic film.

Twenty-four hours after the adhesive cementation of the abutments, the specimens were placed on as many radiographic films (4.1 mm × 3.1 mm) (Ultra Speed, Kodak, USA) before being irradiated for 0.14 s with a radiographic device at a voltage of 70 kV and an electric intensity of 15 mA (X70, Castellini, Italy) sets to a focal distance of 25 cm from the film. The radiographic films have been developed and fixed with standard technique, and subsequently, have been digitally acquired through a flatbed scanner with a resolution of 1200 dpi (Epson Perfection V700 Photo Scanner, Epson, Japan).

Afterward, according to a research protocol, all specimens have been submitted to three series of fatigue cyclic loading. Every series of loading consisted of 200,000 cycles of sinusoidal load applied with a frequency of 2 Hz. The first series had a maximum compressive load of 140N and a minimum load of 15N. The second series had a maximum compressive load of 190N and a minimum load of 19N. The third series had a maximum compressive load of 340N and a minimum load of 34N. To perform the fatigue test, the specimens were placed in a gripping system with an inclined plane of 30°.

The fatigue testing machine used for the experimentation was a pneumatic instrument (Lloyd-SiPlan, Lloyd Instruments Ltd., UK) equipped with a load cell of 5 kN and a computer with a dedicated managing software (Lloyd-SiPlan servant-controller, Lloyd Instruments Ltd, UK) [Figure 2].

After every series of loading, the specimens have been X-rayed and digitally acquired again with the purpose to underline possible micro-movements of the abutment [Figure 3]. The images have been submitted to digital analysis by means of a specific software (Image Pro Plus 4.1, Media Cybernetics, USA), for a quantitative evaluation of possible abutment micro-movements against the fixture. For this purpose, the distances between the right and left bottom limit of the brass cup and the homologous limit of the profile of the first fixture coil have been measured [Figure 4] on each radiographic image. Four pairs (right and left side) of measurements were so obtained for each specimen (start; 1st cycle; 2nd cycle; 3rd cycle). Subsequently, the difference has been calculated (Δx), between the first pair of measurements and those following the application of the cyclic load, in order to obtain a mean value and a standard deviation of the Δx, for each specimen and for both sides in every single cycle of loading.

The condition of each abutments has been evaluated at the end of the third and the last cycle of loading and a score has been assigned, according to the presence (score = 1) or absence (score = 0) of the following phenomena: Abutment debonding; visible deformation of the abutment; fracture of the abutment.

Then, the results have been statistically analyzed through the Mann–Whitney's U-test, for the comparison between the two groups and the Wilcoxon signed-rank test for the observations before and after the treatment within the samples of the same group.

The excursion that the two types of abutments suffered, during the application of the three different intensities of sinusoidal load, was evaluated in order to assess the potential capacity of the TCFRA in mitigating the tensile and divergent components transmitted to the bone in the case of an transverse load to the fixture. The analysis was conducted on 10 abutments (5 for each group, randomly chosen) at the beginning of each test of cyclic stress for 5 min. The swinging was monitored by a digital camcorder mounted on a tripod (Sony HRD-HC1E PAL, Sony Inc., Japan). The videos were acquired in the HDV format (1080i/miniDV, 25 frames/s). Using a video editing software (Pinnacle Studio Plus 9.4.3, Pinnacle Systems Inc., USA), it was possible to analyze and capture individual frames (BMP format, resolution 1440 × 1080) coinciding with the limit positions of the sinusoidal curve corresponding to the load (upper and lower limit of the load). The images thus obtained were processed by means of a digital image analysis software (Image Pro Plus 4.1, Media Cybernetics, USA). In order to quantify the excursion of the abutment and to calibrate the digital image analysis software, a grid graph was used [Figure 5]. The grid was adjacent to the sample that resulted so interposed between this and the camcorder. The frames, coinciding with upper and lower limits of the load, were then compared measuring the excursions showed by the anterior-superior edge of the coping cylindrical brass cup against a fixed reference point chosen on the grid graph [Figure 6]. The swinging values, for each range of stress
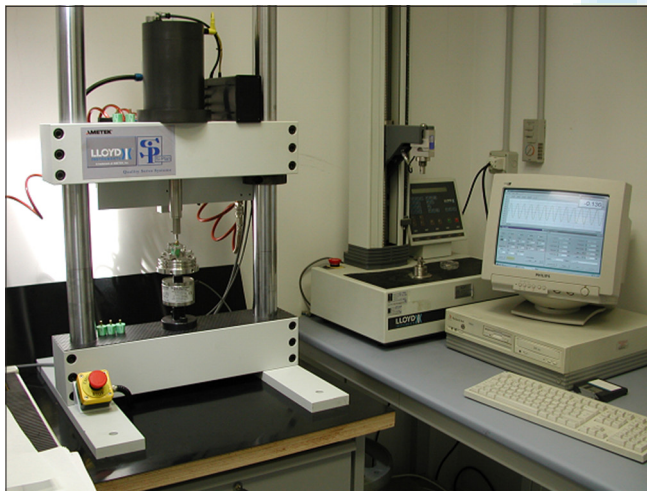

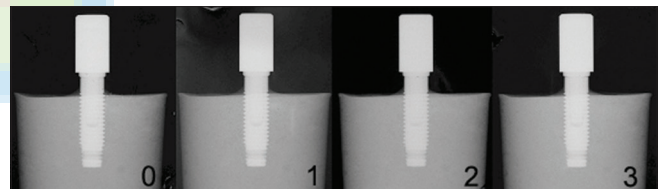**Figure 2:** The pneumatic device used for the cyclical solicitation

Figure 3: X-ray of a sample: 0 = before fatigue tests, 1 = after the first cycle, 2 = after the second cycle, 3 = after the third cycle
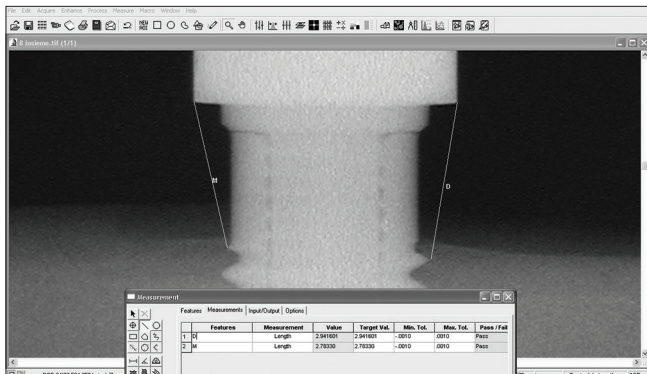

Figure 4: Measure of possible micro-movements on every radiographic image by means a specific software
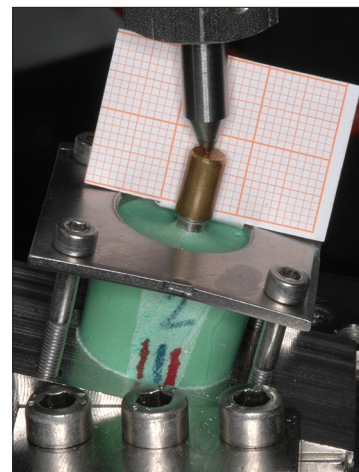

Figure 5: A specimen during the cyclical solicitation. A grid graph was used adjacent to the sample in order to quantify the excursion of the abutment and to calibrate the digital image analysis software

chosen, were compared, within each group and among the groups, using the Student–Newman–Keuls test.

RESULTS

Four specimens in the TA group presented the debonding of the abutment without apparent structural failures, with the only exception of one specimen that showed a visible deformation of the abutment associated to debonding. One specimen displayed a fracture of the TA toward the end of the third cycle of solicitation (195,470 cycles), the fracture occurred orthogonally involving the long vertical axis of the abutment, at the level of the contact point with the neck of the fixture [Figure 7].

In TCFRA group, three specimens presented the debonding of the TCFRA without revealing structural failures.

As regards the TA group, both the fracture and the deformation of the abutment occurred in 12.5% of cases; the debonding in 62.5% of cases. In the TCFRA group, the only issue observed was the debonding of the abutment in 37.5% of cases.

In spite of the reduced number of specimens, the Wilcoxon signed-rank test shows that there is not a statistically significant difference within the TA group concerning the debonding ($P < 0.062$), after the cyclical loading, while in the TCFRA group, it is not possible to achieve any statistic result, due to sample limits.

The comparison between the groups through the Mann–Whitney's U-test shows a not significant difference ($P > 0.06$).

As regards micro-movements around two sides M (left) and D (right) of each abutment, it is possible to remark that the positive Δx values are related to situations of extrusion of the abutment from the fixture, while those with negative Δx values are related to the intrusion of the abutment in the fixture [Tables 1 and 2]. In the TCFRA group, 24 couples of Δx values were calculated while in the TA group the couples of Δx values were 23, since one specimen was fractured toward the end of the third cycle of loading. As regards micro-movements exhibited during cyclic loading, in the TA group, the extrusion was more present (78.3% side M; 56.5% side D), while in the TCFRA group the intrusion was more frequent (70.8% side M; 62.5% side D) [Table 3]. The absence of micro-movements was exhibited in both groups, on the same side (M), in two cases only: A TA after the second cycle of loading [Table 1]; a TCFRA after the first cycle of loading [Table 2]. The size of the extrusions is greater in both sides, in comparison to the intrusions, in the TA group [Table 3]. The size of the extrusions is lower in sides M and greater in sides D in the TCFRA group while the intrusions exhibit a comparable size on both sides [Table 3].
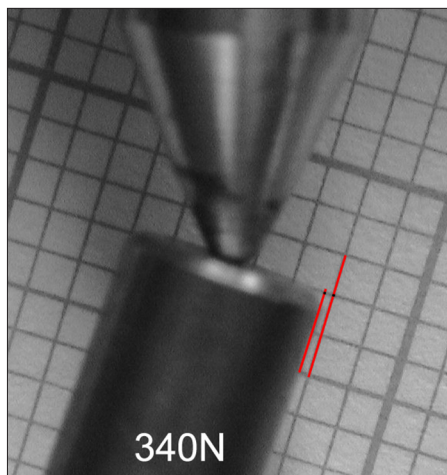
Figure 6: The frames, coinciding with upper and lower limits of the load, were compared measuring the excursions showed by the anterior-superior edge of the coping cylindrical brass cup against a fixed reference point chosen on the grid graph
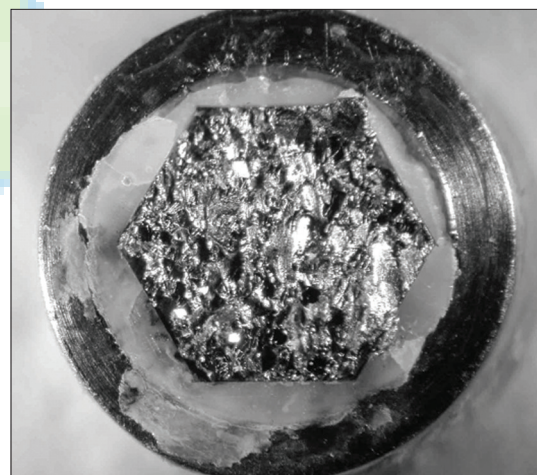
Figure 7: Frame, coinciding with upper limit of the load, the excursion was measured in the same manner of figure 6

Table 1: Micro-deformation exhibited, in titanium abutments group, after every solicitation cycle

Specimen	Titanium abutments group					
	Side M Δx (mm)			Side D Δx (mm)		
	1^ cycle	2^ cycle	3^ cycle	1 ^cycle	2^ cycle	3^ cycle
1	0.047	0.004	0.028	−0.039	−0.038	−0.019
2	0.057	0.038	0.061	0.016	0.038	0.103
3	−0.02	−0.035	0.054	0.042	0.014	0.01
4	0.013	0.007	0.111	−0.033	−0.014	0.008
5	0.111	0.089	−0.012	0.005	0.002	−0.006
6	−0.031	−0.019	0.077	−0.003	−0.003	−0.003
7	0.077	0.073	0.003	0.017	−0.005	0.042
8	0.003	0		0.045	0.045	
mean	0.032	0.020	0.046	0.006	0.005	0.019
st dev	0.049	0.044	0.043	0.031	0.027	0.042

Concerning the swinging showed by the two types of abutment during the solicitation, in TAs, the swinging was 2.4 µm (±0.2), 6.1 µm (±0.3), 22.7 µm (±0.7), respectively, in the three intervals of increasing compressive load applied, while in the case of the TCFRAs, the swinging was 57.8 µm (±2.7), 89.9 µm (±1.5), and 115.6 µm (±3.1), respectively, in the above-mentioned three intervals [Table 4]. Student–Newman–Keuls test showed a significant difference within the TCFRA group and between the 2 groups ($P < 0.05$), with the exception of the swinging exhibited by the TAs, as a result of the first and second cyclic stress ($P > 0.05$). On the other hand, the oscillation resulting from the third cycle of solicitation was significantly higher than the ones exhibited during the two previous cycles ($P < 0.05$).

DISCUSSION

One of the etiological causes of crestal bone resorption, in conditions of load, is represented by the excessive stress transmitted to the bone-implant interface.[1] The titanium has an elastic modulus about 5 times higher than that of cortical bone, and this facilitates the concentration of stress at the level of the crestal bone.[9-11] The PL that surrounds the natural tooth works as a viscoelastic shock absorber, able to reduce the flow stress to the crestal bone, thus lengthening the time in which the load is dissipated.[2,3] The adoption of a flexible abutment could help in this way. In fact, due to its anisotropic nature, the TCFRA deforms itself, within its elastic limit, absorbing part of the applied load. Hence, the higher flexibility, exhibited by this experimental abutment, could theoretically prevent the excessive concentration of stress in the implant-bone interface. Apparently, the TCFRA exhibits marked viscoelastic properties certainly useful in the dissipation of chewing loads, especially if the stresses are not parallel to the axis of the fixture. The use of this type of abutments could be beneficial not only in normal situations but also in the case of parafunctional habits such as clenching and bruxism.

The lower percentage rate of debonding exhibited by TCFRAs (37.5% vs. 62.5%) could be attributed to the experimental nature of their resinous matrix that makes them more likely to bond the composite resin cement. Furthermore, their greater intrinsic roughness could have a role in this phenomenon.

The high rate of extrusion exhibited by TAs could be attributed to the debonding consequent to cyclical solicitation.

The prevalence of intrusion into the TCFRA group is probably due to the anisotropic structure of the abutment. In fact, the orientation of the fibers gives a higher elasticity in bending and a lower resistance under compression if compared to TA. The intrusive behavior of the TCFRA could theoretically avoid the crestal bone resorption in the case of occlusal overload. In fact, the natural teeth exhibit a greater ability to perceive any interference respect to implant-supported prosthetic teeth.[4,5] Furthermore, the latter perceive noxious stimuli (pressure) in a delayed and attenuated manner if compared to natural teeth, which are known to have a quicker and acute response.[4,5]

Table 2: Micro-deformation exhibited, in TCFRAs group, after every solicitation cycle

| Specimen | TCFRAs group | | | | | |
| | Side M Δx(mm) | | | Side D Δx(mm) | | |
	1^ cycle	2^ cycle	3^ cycle	1^ cycle	2^ cycle	3^ cycle
1*	0.006	0.006	0.01	−0.025	−0.03	−0.022
2*	−0.03	−0.008	−0.019	−0.003	−0.029	−0.018
3*	−0.012	−0.016	0.003	−0.035	−0.015	−0.046
4*	−0.005	−0.044	−0.019	0.024	0.057	0.038
5*	−0.032	−0.021	0.019	−0.038	−0.007	0.019
6*	0	0.007	−0.006	−0.002	0.006	−0.019
7*	−0.038	−0.038	−0.005	−0.058	−0.061	0.013
8*	−0.016	−0.031	−0.016	0.039	0.078	0.078
mean	−0.016	−0.018	−0.004	−0.012	0.000	0.005
st dev	0.016	0.019	0.014	0.033	0.046	0.040

Table 3: Extrusion and intrusion showed in both groups. The values in brackets indicate the number of times that a particular behaviour occurred on the two different sides

	Titanium abutments group				TCFRAs group			
	Δx (mm)				Δx (mm)			
	Extrusions		Intrusions		Extrusions		Intrusions	
	Side M (17)	Side D (13)	Side M (5)	Side D (10)	Side M (6)	Side D (9)	Side M (17)	Side D (15)
mean	0.047	0.030	−0.023	−0.016	0.009	0.039	−0.021	−0.027
st dev	0.038	0.027	0.009	0.015	0.006	0.027	0.012	0.018

Table 4: Swinging recorded, in both groups, at the beginning of each solicitation cycle

| Specimen | Titanium abutments group | | | Specimen | TCFRAs group | | |
| | Swinging (µm) | | | | Swinging (µm) | | |
	14-140N	19-190N	34-340N		14-140N	19-190N	34-340N
1	2.4	6.3	22.7	1*	61.5	87.8	115.8
2	2.3	6.1	22.6	2*	55	90.6	118.2
3	2.2	6.4	23.8	3*	57	91.7	116.3
4	2.6	5.7	21.7	4*	55.8	89.3	110.3
5	2.7	6.1	22.5	5*	59.6	90	117.6
mean	2.440	6.120	22.660	mean	57.780	89.880	115.640
st dev	0.207	0.268	0.750	st dev	2.711	1.458	3.137

In both groups, the failure of the adhesive bond occurred at the cement-abutment interface, probably due to the cemented portion of the abutment, did not have a satisfactory macro-retentive structure at the inner surface of the fixture that was instead threaded.

The trend toward the debonding in the TAs can probably be reduced by means of thin transverse grooves, at the level of their cemented portion, in order to obtain a valid macro-retentive structure. Even the tendency toward the debonding in TCFRAs can be reduced in a similar manner. Despite both the composite cement and the adhesive system used are particularly suitable for the cementation of passivated metals and fiber posts, a further development of adhesive systems and composite cements, specific for coupling the titanium with this type of experimental abutment, could contribute to improve the quality and duration of the bond.

The experimental abutments theoretically exhibit the best aesthetic properties, avoiding the shining effect associated with metal abutments. For this reason, they could be advantageous associated with full ceramic crowns.

Considering that in clinical conditions the TCFRA comes in close contact with the soft tissues and the oral environment, in general, at the present state, it is unknown if such device can affect the deposition and the development of microbial plaque on its surface, as well as its soft tissues response. Due to the small sample size, the present study provides preliminary results of a trend related to mechanical properties of resin glass fiber-reinforced abutment in comparison to TA. Additional studies with larger samples will be helpful to confirm our results.

REFERENCES

1. Pesqueira AA, Goiato MC, Filho HG, Monteiro DR, Santos DM, Haddad MF, *et al.* Use of stress analysis methods to evaluate the biomechanics of oral rehabilitation with implants. J Oral Implantol 2014;40:217-28.
2. Pektas Ö, Tönük E. Mechanical design, analysis, and laboratory testing of a dental implant with axial flexibility similar to natural tooth with periodontal ligament. Proc Inst Mech Eng H 2014;228:1117-25.
3. Simamoto Júnior PC, da Silva-Neto JP, Novais VR, de Arruda Nóbilo MA, das Neves FD, Araujo CA. Photoelastic stress analysis of mandibular fixed prostheses supported by 3 dental implants. Implant Dent 2014;23:704-9.
4. Machtei EE, Oettinger-Barak O, Horwitz J. Axial relationship between dental implants and teeth/implants: A radiographic study. J Oral Implantol 2014;40:425-31.
5. Marchetti E, Ratta S, Mummolo S, Tecco S, Pecci R, Bedini R, *et al.* Evaluation of an endosseous oral implant system according to UNI EN ISO 14801 fatigue test protocol. Implant Dent 2014;23:665-71.
6. Cidade CP, Pimentel MJ, Amaral RC, Nóbilo MA, Barbosa JR. Photoelastic analysis of all-on-four concept using different implants angulations for maxilla. Braz Oral Res 2014;28(1):1-7.
7. Tanasic I, Tihacek-Sojic L, Milic-Lemic A. Finite element analysis of compressive stress and strain of different implant forms during vertical loading. Int J Comput Dent 2014;17:125-33.
8. Jindal S, Bansal R, Singh BP, Pandey R, Narayanan S, Wani MR, *et al.* Enhanced osteoblast proliferation and corrosion resistance of commercially pure titanium through surface nanostructuring by ultrasonic shot peening and stress relieving. J Oral Implantol 2014;40:347-55.
9. Brunski JB. Biomechanical aspects of the optimal number of implants to carry a cross-arch full restoration. Eur J Oral Implantol 2014;7 Suppl 2:S111-31.
10. Moreira W, Hermann C, Pereira JT, Balbinoti JA, Tiossi R. A three-dimensional finite element study on the stress distribution pattern of two prosthetic abutments for external hexagon implants. Eur J Dent 2013;7:484-91.
11. Carvalho MA, Sotto-Maior BS, Del Bel Cury AA, Pessanha Henriques GE. Effect of platform connection and abutment material on stress distribution in single anterior implant-supported restorations: A nonlinear 3-dimensional finite element analysis. J Prosthet Dent 2014;112:1096-102.
12. Zarb GA. On parafunctional considerations in implant therapy. Int J Prosthodont 2014;27:199.
13. Keenan AV, Levenson D. Are ceramic and metal implant abutments performance similar? Evid Based Dent 2010;11:68-9.
14. Nakamura K, Kanno T, Milleding P, Ortengren U. Zirconia as a dental implant abutment material: A systematic review. Int J Prosthodont 2010;23:299-309.
15. Santiago Junior JF, Pellizzer EP, Verri FR, de Carvalho PS. Stress analysis in bone tissue around single implants with different diameters and veneering materials: A 3-D finite element study. Mater Sci Eng C Mater Biol Appl 2013;33:4700-14.
16. Gehrke SA, Pereira Fde A. Changes in the abutment-implant interface in Morse taper implant connections after mechanical cycling: A pilot study. Int J Oral Maxillofac Implants 2014;29:791-7.
17. Behr M, Lang R, Leibrock A, Rosentritt M, Handel G. Complication rate with prosthodontic reconstructions on ITI and IMZ dental implants. Internationales team für implantologie. Clin Oral Implants Res 1998;9:51-8.
18. Bitter K, Kielbassa AM. Post-endodontic restorations with adhesively luted fiber-reinforced composite post systems: A review. Am J Dent 2007;20:353-60.
19. Rosentritt M, Behr M, Lang R, Handel G. Experimental design of FPD made of all-ceramics and fibre-reinforced composite. Dent Mater 2000;16:159-65.